

U11561

UNITED STATES ATOMIC ENERGY COMMISSION

AECD-2848

TOTAL CROSS SECTIONS OF NUCLEI FOR 280
MEV NEUTRONS - I

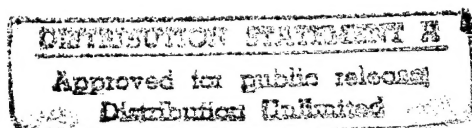
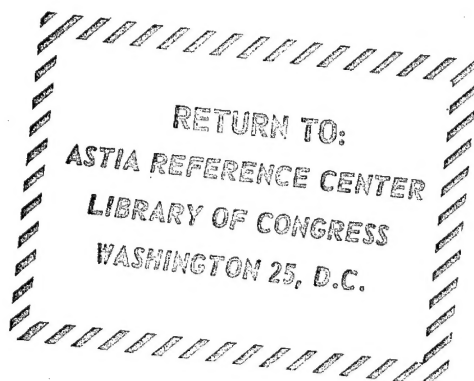
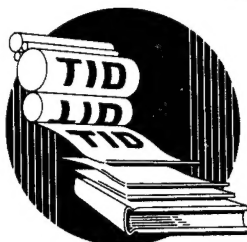
By
R. Fox et al.

NAVY RESEARCH SECTION
SCIENCE DIVISION
REFERENCE DEPARTMENT
LIBRARY OF CONGRESS

10
SEP 29 1950

January 26, 1950

University of California
Radiation Laboratory



Technical Information Division, ORE, Oak Ridge, Tennessee

19960724 113

50
my

DTIC QUALITY INSPECTED 3

Issuance of this document does not constitute
authority for declassification of classified
copies of the same or similar content and title
and by the same authors.

Styled, retyped, and reproduced from copy
as submitted to this office.

PRINTED IN U.S.A.
PRICE 10 CENTS

TOTAL CROSS SECTIONS OF NUCLEI FOR 280-MEV NEUTRONS - I*

R. Fox,[†] C. Leith,[†] L. Wouters,[†] and K. R. MacKenzie[‡]

ABSTRACT

The measurement of 280-Mev neutron cross sections of various nuclei is described. The neutron beam used results from 340-Mev protons in the 184-in. cyclotron striking a 2-in. Be target. The neutron detector consists of a double coincidence anthracene scintillation counter telescope which counts recoil protons scattered at 15 deg from a paraffin cylinder placed in the collimated neutron beam. A 2-in. Cu absorber placed between the counters assures that only protons of energy greater than 250 Mev are counted. The cross sections for all nuclei measured from Li to Pb are smaller than the corresponding cross sections measured at 90 Mev¹ by factors between 0.5 and 0.6.

INTRODUCTION

When the total cross sections of various elements for 85-Mev neutrons were measured a year ago¹ it was noticed that elements of low atomic weight behaved as if they were at least partially transparent. Therefore, when the 280-Mev neutron beam became available after conversion of the 184-in. cyclotron, it was considered advisable to examine this effect at the higher energy. The measurements also would add to our knowledge of the fundamental properties of nuclei; a correct theory should be able to predict these cross sections and their functional dependence upon energy and atomic number in an unambiguous manner. Conversely, knowledge of these values may furnish additional clues leading to the correct nuclear model. These measurements were made using two independent detection methods. Measurements made using scintillation counters are described in Part I of this report, and measurements made using bismuth fission counters are described in Part II.

*Work performed under Contract No. W-7405-eng-48.

[†]Radiation Laboratory, Department of Physics, University of California, Berkeley, California.

[‡]Department of Physics, University of California at Los Angeles, California.

SOURCE OF NEUTRONS

The neutron beam used for these measurements was produced by bombarding a 2-in. thick beryllium target in the cyclotron vacuum chamber with 350-Mev protons. Charge exchange leads to the production of a neutron beam of about 270-Mev mean energy and angular width at half maximum intensity of about 58 deg. The central forward section of this beam was selected, first by a collimating system consisting of a $\frac{1}{2}$ -in. hole through a 7-ft-cube of concrete placed between the cyclotron and the surrounding concrete shielding wall, and second by means of an exchangeable steel plug with any desired aperture inserted into a 3-in. hole in the 10-ft shielding wall itself. In this experiment, a $2\frac{5}{8}$ by $1\frac{3}{8}$ -in. aperture was employed.

The energy distribution of the neutron beam was obtained by measuring the range distribution, and hence deducing the energy distribution, of recoil protons from hydrogen, at a fixed angle with respect to the beam. The range-energy curves used were calculated from the theoretical formula of Livingston and Bethe² using $I = 11.5Z$ ev. Paraffin and carbon scatterers were used alternately to obtain the hydrogen difference. The range distribution was determined by varying the absorber thickness between two scintillation counters in coincidence and counting the recoil protons as illustrated in Fig. 1. To each thickness there corresponds a minimum proton energy E_{p1} for penetration, so that all protons with energy $E_p = E_{p1}$ passing through both counters were counted. This number is proportional to the number of neutrons of energy $E_n > E_{n1} = \frac{E_{p1}}{\cos^2 \theta}$, θ being the laboratory scattering angle with respect to the forward direction.

There is one serious difficulty. At these energies, the absorber thickness required is an appreciable fraction of a mean free path for a nuclear encounter, so that a fraction of the protons of energy $E_p > E_{p1}$ are not counted. If the cross section for these processes which remove protons were known, an accurate correction could be made; however, only an estimated correction is possible at present.

Incorporating this estimated correction and differentiating the resulting distribution, it is found to have a peak at 270 Mev (± 15 Mev) with an estimated width of 30 Mev as shown in Fig. 2.

METHOD

Principle

To measure the total cross sections of various elements for high energy neutrons, use is made of the exponential decrease in intensity of a mono-energetic beam in the forward direction as the thickness of matter traversed (X) is increased:

$$I(X) = I(0)e^{-X/\lambda}$$

where λ is the mean free path, related to the total cross section by:

$$1/\lambda = N \rho / A \sigma_t$$

N being Avogadro's number, ρ the density, and A the atomic weight. Then the total cross section is:

$$\sigma_t = A/N\rho X \ln \left[\frac{I(0)}{I(X)} \right]$$

Numbers proportional to the beam intensities $I(0)$, $I(X)$ are obtained by counting the recoil protons generated at a fixed angle (usually 15 deg) by a small paraffin cylinder placed in the neutron beam behind the samples. The recoil protons were counted by means of two scintillation counters in coincidence in much the same way as described above.

This paraffin proton generator was placed in the neutron beam 12 ft from the last collimator; the sample, about one mean free path in length and 3 in. in diameter, was placed in the beam 2 ft from the last collimator. A BF_3 slow-neutron counter was located in a hole in the concrete wall adjacent to that collimator for monitoring purposes. With these arrangements the ratio $R(X)$ of detector to monitor counting rates is proportional to $I(X)$, a second ratio $R(0)$, proportional to $I(0)$, is obtained by removing the sample. When these ratios are corrected for background, we get new ratios $R'(0)$, $R'(X)$. Then,

$$\frac{I(0)}{I(X)} = \frac{R'(0)}{R'(X)}$$

Counter

The individual scintillation counters (see also Fig. 1) consisted of uniform anthracene crystals $\frac{3}{16}$ in. thick and 1 sq. in. in area mounted in light-tight polished aluminum boxes, each in turn facing a 1P21 photomultiplier tube. Two such units were mounted as a coincidence telescope looking at the paraffin recoil proton generator at 15 deg laboratory angle. In order to confine coincidences to protons generated by high energy neutrons, a 2-in. Cu absorber was placed between the crystals, thus providing an equivalent neutron threshold of 250 Mev.²

The geometry was arranged so that the path of the counted recoil protons passes normally through the crystals and through a uniform, known thickness of aluminum. Fast (10^{-8} sec) light pulses were produced due to the excitation and subsequent fluorescence induced in the anthracene by the protons. The photomultipliers convert these into electric signals which are further amplified and mixed in a coincidence circuit. This system has a 0.25 μsec resolving time. The output was counted by a standard scaler.

When plotting counting rate versus photomultiplier voltage (or gain), a flat plateau is observed as shown in Fig. 3, corresponding to the detection of virtually all protons, but no other particles. Above this proton plateau γ rays, β particles, noise, etc., begin to be counted. Since the plateau width is 300 volts (corresponding to a gain ratio of about 8), constant

detector efficiency is assured by setting the photomultiplier voltage at its center.

Monitor

The BF_3 monitor counted slow neutrons leaking through the concrete from the collimator. Since the background flux was several orders of magnitude smaller than the slow neutron flux originating at the collimator, its counting rate was satisfactorily proportional to the latter. This monitor was shielded from backscattering by a 2-ft Cu plug between it and the sample. The chief problem with such a monitor is the finite slope and narrow width of its plateau, in contrast to the wide, flat plateau of the scintillation counters. Accordingly very good voltage regulation must be provided or the efficiency will vary. Any significant variations due to this or other causes affecting the entire experiment can be checked by a statistical analysis of groups of counts.

Technique

(a) Alignment. The equipment was mounted in such manner as to permit accurate centering of the paraffin generator in the neutron beam. This alignment was checked by means of a cathetometer previously aligned with the inner collimator and the central point of emergence of the neutron beam at the vacuum tank. Likewise, the alignment of the samples could be similarly checked to see that no neutron path could reach the generator without passing through the sample.

In operation, the counting rate is maximized as a function of cyclotron target position to ensure that the beam is not emerging obliquely. The entire alignment was further checked by exposing film in the beam, at the generator.

(b) Geometry. The beam area was 3.6 sq in. and the sample to generator distance varied from 7 to 9 ft, depending on sample length. This gives a solid angle of from 3×10^{-4} to 5×10^{-4} steradian, which is sufficiently "good" to avoid scattering correction in case of the light elements. For the heavy elements, a small scattering correction is necessary.

(c) Accidental Coincidences. Background. During early runs, the coincidence counting rate was of the order of 3 cps with single counting rates of $N_1 \sim 800$ cps in the first counter and $N_2 \sim 150$ cps in the second counter. Calling the accidental coincidence rate N_c and using the relation $N_c = 2N_1N_2 \tau A$, where τ is the resolving time of $0.25 \mu\text{sec.}$ and A (~ 300) is the reciprocal beam duty factor, we get $N_c \sim 0.06$ cps. This is about 2 per cent of the observed total coincidence rate. Therefore, for later runs, N_c was measured experimentally by placing sufficient absorber between the crystals to eliminate true coincidences. The beam intensity was then reduced until N_c was less than 0.5 per cent of the total coincidence rate.

The principal source of background was due to diffracted neutrons reaching the first crystal directly and there producing recoil protons which were counted. With the sample in place, these neutrons came from the sample. With the sample removed, they came from the iron collimator. This background

was measured directly before and after all runs by removing the paraffin proton generator and determining the coincidence rate. This was done with the sample in place and with the sample removed. Detector to monitor ratios thus obtained were subtracted from the ratios $R(X)$ and $R(O)$ to yield $R'(X)$ and $R'(O)$.

In order to check for other sources of background, the following experiment was performed. First, a run was made with one mean free path of carbon and 24 in. of lead as the sample and with the paraffin in place. A second run was made with the paraffin removed. Then a third run was made with both paraffin and lead removed. Normalizing the coincidence counts to equal monitor counts, the following numbers were obtained: 1st run, 12 counts; 2nd run, 6 counts; and 3rd run, 92 counts.

The first setup detects diffracted neutrons which pass through several mean free paths of sample to the first crystal, neutrons scattered by air around the sample into the first crystal, neutrons scattered by air around the sample into the paraffin, and neutrons from the beam which reach the paraffin through about seven mean free paths of sample. The second setup detects only the first and second of these. The third setup detects neutrons scattered by air around the sample into the first crystal and diffracted neutrons which have passed through less than a mean free path of sample on the average and then reach the first crystal of the counter.

While the difference between the first two runs is not statistically significant, it is about what one would expect due to attenuation of the beam in the sample. Comparison of these runs with the third one shows the background due to beam neutrons scattered around the sample into the paraffin is negligible compared to that due to diffracted neutrons reaching the first crystal. The latter is just the background measured for all runs.

The background correction thus measured ranged from less than 1 per cent for light elements up to 10 per cent for heavy elements. It was proportional to the total cross section of the sample used as would be expected if it were caused by diffracted neutrons.

Another check on accidental coincidence rate was made at the beginning of all runs by checking linearity of counting rate with beam intensity. This also proved to be a critical check on equipment performance and in addition showed that the factors of proportionality $R'(X)/I(X)$ and $R'(O)/I(O)$ must be the same.

(d) Counting. Since long runs were needed to obtain cross section values with reasonable accuracies, it was not feasible to repeat each run many times. Instead, they were broken up into short equal periods, so that any significant drifts could be noticed. $R(O)$ and $R(X)$ were calculated, both for each short run and for the entire group, together with their statistical error and standard deviation. In only one case did the fraction of short runs lying outside the standard error of the mean exceed the expected 30 per cent. In that case, a monitor voltage drift was found, and the run discarded.

(e) Samples. With the exception of lithium and uranium, all samples were 3 in. in diameter and about one mean free path long. Liquids were held in brass cylinders 3 in. in diameter of appropriate length, having $\frac{1}{16}$ in. walls; empty cylinders were used for the blank run. In the case of lithium,

the 2 in. square blocks already available were employed.¹ The uranium cylinder was about 2 in. in diameter, so that a smaller beam collimator was used, and an individual film exposure made to insure that it intercepted all of the beam.

Hydrogen was done by a difference method, using pentane and carbon; this gave both σ_H and σ_C . The deuteron cross section was done by a similar method using water and heavy water; this gave σ_D and σ_O , using σ_H determined above. Such procedures lead to reduced accuracy, so that the purity, density, and dimensions of all these materials were checked. For all samples used, the thickness (in gm/cm²) was established to better than 1 per cent, in most cases to 0.2 per cent.

(f) Scattering Correction. For elements of high atomic weight, a small correction for neutron scattering is necessary. This was calculated in the manner of Cook, McMillan, et al.¹

The values of the various constants are:

$$a = 1.5 \text{ in.}$$

$$k = 3.94 \times 10^{13}/\text{cm}$$

$$x_1 = 100 \text{ in.}$$

$$x_2 = 480 \text{ in.}$$

It turns out fortuitously that the correction to the cross section in per cent is just the value of the cross section in "barns," except for uranium, for which the correction was 1.5 per cent.

DISCUSSION OF RESULTS

The results are tabulated in Table 1 together with the 90-Mev results¹ for comparison. The errors are those computed from counting statistics alone.

At present, no nuclear model theories fit these data very well. The results of Cook, McMillan, et al, at 90 Mev show a nuclear transparency in terms of a "mean free path within the nucleus."³ They also show agreement with the consequent prediction that the transparency should be greatest for elements of low atomic weight, as shown by the deviation from a straight line in Fig. 4. However, at 280 Mev, the transparent nucleus theory predicts a higher cross section for elements of high atomic weight than is actually observed.

ACKNOWLEDGMENT

The group wishes to thank Professor E. O. Lawrence for suggesting and encouraging the work, and members of the Laboratory for assistance.

Table 1--Total Cross Sections at 280 Mev
with Those at 85* Mev Included for Comparison†

Element	A	A ^{1/3}	280 Mev				85 Mev			
			$\sigma \times 10^{24} \text{cm}^2$	$\sqrt{\frac{\sigma}{2\pi}} \times 10^{13} \text{cm}$	$\sigma \times 10^{24} \text{cm}^2$	$\sqrt{\frac{\sigma}{2\pi}} \times 10^{13} \text{cm}$	$\sigma \times 10^{24} \text{cm}^2$	$\sqrt{\frac{\sigma}{2\pi}} \times 10^{13} \text{cm}$	$\sigma \times 10^{24} \text{cm}^2$	$\sqrt{\frac{\sigma}{2\pi}} \times 10^{13} \text{cm}$
H ¹	1.008	1.00	0.033 ±0.003	0.725 ±0.04	0.083 ±0.004	1.15				
H ²	2.015	1.26	0.049 ±0.005	0.884 ±0.04	0.117 ±0.005	1.36				
Li	6.940	1.91	0.164 ±0.007	1.62 ±0.04	0.314 ±0.006	2.24				
Be	9.02	2.08	0.225 ±0.004	1.89 ±0.02	0.431 ±0.008	2.26				
C	12.01	2.29	0.279 ±0.004	2.11 ±0.01	0.550 ±0.011	2.96				
O	16.00	2.52	0.380 ±0.008	2.46 ±0.03	0.765 ±0.020	3.49				
Al	26.97	3.00	0.566 ±0.018	3.00 ±0.05	1.12 ±0.02	4.22				
Cu	63.57	3.98	1.19 ±0.02	4.35 ±0.04	2.22 ±0.04	5.95				
Sn	118.7	4.92	1.83 ±0.03	5.40 ±0.11	3.28 ±0.06	7.23				
Hg	200.6	5.85	2.80 ±0.03	6.69 ±0.11						
Pb	207.2	5.92	2.89 ±0.03	6.79 ±0.10	4.53 ±0.09	8.49				
U	238.1	6.20	3.14 ±0.05	7.02 ±0.21	5.03 ±0.10	8.95				

*Later considerations have shown that the mean detection energy was actually 85 Mev and not 90 Mev as stated in Reference 1.

†Errors are calculated from counting statistics alone.

REFERENCES

1. Cook, McMillan, et al, Phys. Rev., 75: 1 (1949).
2. Bethe, Rev. Mod. Phys., 9: 263 (1937), Eq. 9.263.
3. Fernbach, Serber, et al, Phys. Rev., 75: 1352 (1949).

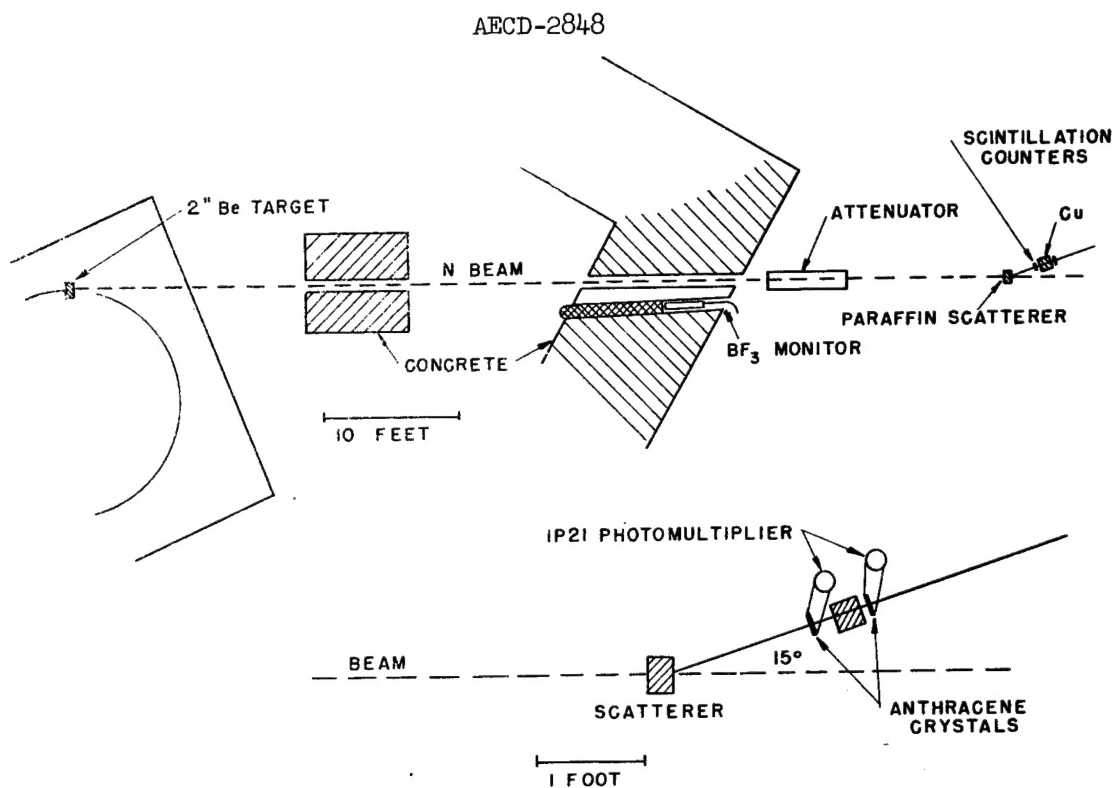


Fig. 1--Schematic diagram representing method of determining proton range distribution.

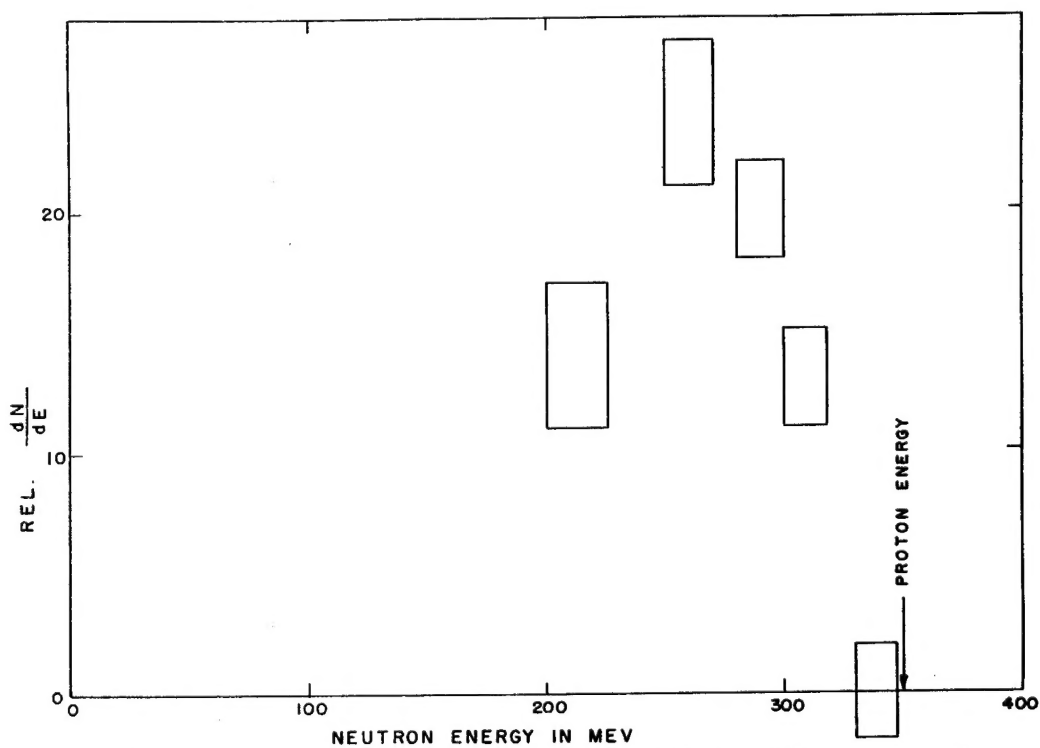


Fig. 2--Neutron beam energy distribution differential range method, 350-Mev proton on 2-in. Be target.

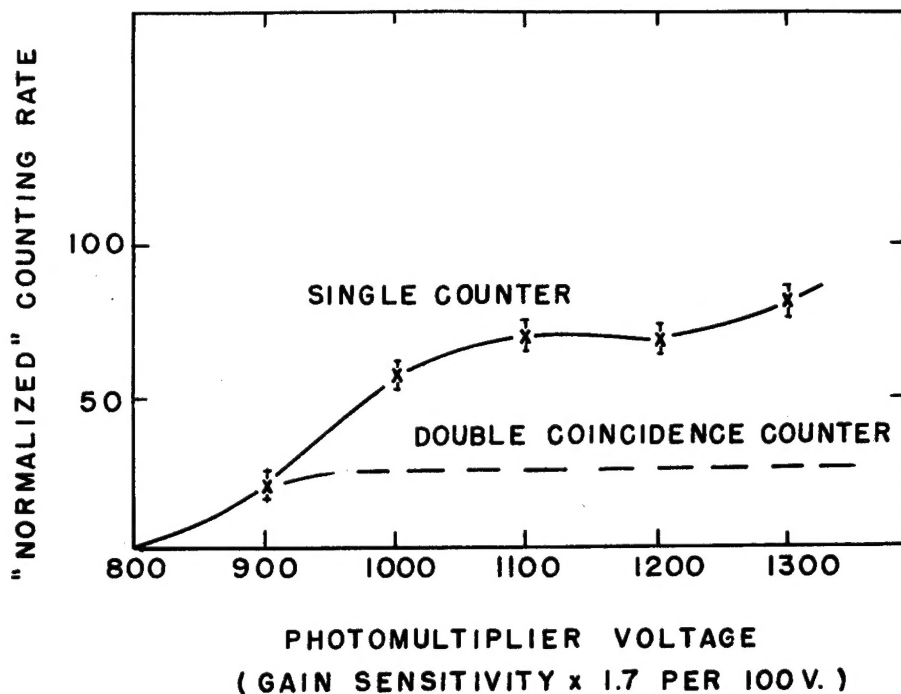


Fig. 3--Curves for single counter and double coincidence counter showing typical proton plateau when photomultiplier voltage is plotted against counting rate.

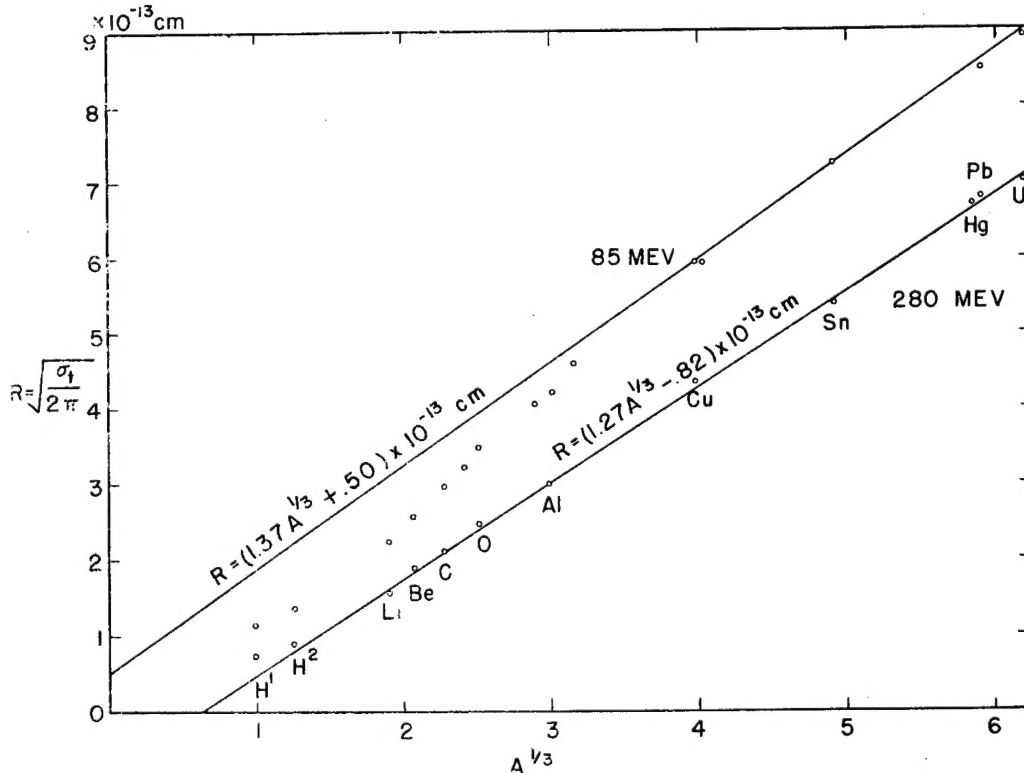


Fig. 4--Comparison of total cross sections at 280 Mev with those at 85 Mev.

END OF DOCUMENT